

See discussions, stats, and author profiles for this publication at: <https://www.researchgate.net/publication/260250732>

Molecular Dynamics Simulation of Electrically Induced Spreading of an Ionically Conducting Water Droplet.

ARTICLE *in* LANGMUIR · FEBRUARY 2014

Impact Factor: 4.46 · DOI: 10.1021/la4044705 · Source: PubMed

CITATION

1

READS

48

3 AUTHORS, INCLUDING:



Fenhong Song

University of Michigan-Dearborn

4 PUBLICATIONS 25 CITATIONS

SEE PROFILE



Chao Liu

Chongqing University

71 PUBLICATIONS 397 CITATIONS

SEE PROFILE

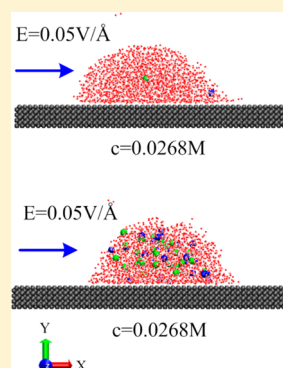
Molecular Dynamics Simulation of the Electrically Induced Spreading of an Ionically Conducting Water Droplet

F. H. Song,[†] B. Q. Li,^{*,‡} and C. Liu^{*,†}

[†]Key Laboratory of Low-Grade Energy Utilization Technologies and Systems of Ministry of Education, Chongqing University, Chongqing 400030, China

[‡]Department of Mechanical Engineering, University of Michigan, Dearborn, Michigan 48128, United States

ABSTRACT: Molecular dynamics simulations are applied to study the spreading behavior of a nanosized water droplet that contains freely moving Na^+/Cl^- ions subject to an imposed electric field parallel to a solid surface. Results show that the positive and negative ions move relatively freely in response to an applied electric field, whereas polar water molecules realign themselves. These localized behaviors of the ions and the polar molecules are affected by both the applied electric field strength and the ion concentration, which in turn determine the deformation and spreading of the droplet on a solid substrate. The presence of the freely moving ions causes the ion-containing droplet to spread differently from a droplet of pure water. In a weak electric field of $0.05 \text{ V}/\text{\AA}$, a droplet of a lower ion concentration spreads asymmetrically and the spreading asymmetry is considerably smaller than that associated with a pure water droplet of the same size. In a stronger field of $0.1 \text{ V}/\text{\AA}$, a droplet of a higher ion concentration spreads symmetrically and completely wets the solid surface whereas a less ionically conducting droplet undergoes an asymmetric-to-symmetric transition in spreading until it reaches equilibrium.



1. INTRODUCTION

Molecular dynamics (MD) simulations provide a useful tool for studying the microscopic mechanism of solid–liquid contact,^{1–7} which is important in understanding phase change phenomena such as the collapse of a film and the dropwise condensation of vapor on a solid surface. With this tool, Blake et al.¹ studied the phenomenon of contact angle relaxation during droplet spreading on a plate and compared the results with the molecular kinetic theory of wetting. Their studies suggest that the dynamic contact angle is not fully described by Young's equation of static stress balance for a macroscopic system. This is consistent with the MD simulations presented by Ingebrigtsen and Toxvaerd.² Guo and Fang³ investigated the dependence of the liquid contact angle on the droplet size and found that the contact angle is sensitive to the interactions between liquid droplets and the solid substrate and decreases as the drop size shrinks for a strong liquid–solid interaction. In addition, the contact angle could be formulated in terms of the surface energy.^{4,5}

Droplet interaction with an external electric field has been a driving mechanism in many microelectronic and nano-optoelectronic technologies, such as electrostatic painting and spraying,^{8,9} inkjet printing,¹⁰ and nanoimprinting and nanomanufacturing.^{11,12} Because of its importance, the subject has been studied by MD simulations,^{13–17} which led to the revelation of novel nanoscale electrowetting effects that were not observed in macroscopic systems. In a recent study, Song et al.¹⁶ also explored the microscopic mechanism on the molecular scale that governs the asymmetric-to-symmetric transition as the spreading of a water droplet on solid surface unfolds under the influence of an applied electric field.

Recently, the electrowetting behavior of ionic liquids has attracted a great deal of attention because of their widespread application as electrowetting agents in many different engineering systems (i.e., digital microfluidic chips,¹⁸ microgrippers,¹⁹ tunable RC filters,²⁰ and variable-focus lenses²¹). Paneru et al.^{22,23} studied the dynamic electrowetting behavior of an ionic liquid droplet in a solid/liquid/liquid system. They observed that viscous dissipation dominated in the system at small dynamic contact angles whereas molecular dissipation prevailed at large contact angles. Li et al.²⁴ investigated the dynamic electrowetting and dewetting process of ionic liquids at a hydrophobic solid–liquid interface. They found that the dynamic contact angle depends on the speed of the contact line and the electrowetting of an ionic liquid was about twice as fast as its retraction. Daub et al.²⁵ used MD simulation to study the salty aqueous nanodroplet spreading on a nonpolar substrate and detected that the contact angle increases with an increase in ion concentration but decreases with an increase in electric field strength whereas the polarity dependence is suppressed in the presence of ions.

Our early studies revealed that a nanosized pure water droplet may spread asymmetrically in an electric field parallel to the solid surface.¹⁶ Information on the electrowetting of an ionically conducting droplet in a parallel field, however, is scarce. This is particularly true for the phenomenon of the asymmetric-to-symmetric transition in electrically induced spreading. This article reports an MD study on sessile

Received: November 19, 2013

Revised: February 10, 2014

Published: February 18, 2014



Table 1. Potential Parameters of the Ion–Ion Interaction

atom	A_{ij}	$10^{79}C_{ij}/\text{J}\cdot\text{m}^6$	$10^{99}D_{ij}/\text{J}\cdot\text{m}^8$	$10^{10}(\sigma_i + \sigma_j)/\text{m}$	$10^9 b_{ij}/\text{J}$	$10^{10}\rho/\text{m}$
Na^+-Na^+	1.25	1.68	0.8	2.34	0.338	0.317
Na^+-Cl^-	1.00	11.20	13.9	2.75	0.338	0.317
Cl^--Cl^-	0.75	116.00	233.0	3.17	0.338	0.317

nanodroplets made up of water and Na^+/Cl^- ions in the presence of an electric field parallel to a solid surface. MD simulations indicate that both the applied field strength and the ion concentration can affect the spreading of an ionically conducting water droplet. The asymmetry between the leading contact angle and the trailing one exists only up to a certain critical value of ion concentration, beyond which the asymmetry disappears and the ionically conducting droplet spreads symmetrically in an electric field.

2. SIMULATION MODEL

A simple point charge/extension (SPC/E)²⁶ water model was used as a basis for MD simulations. The intermolecular interactions between water molecules are calculated as follows. The dispersion and repulsion force uses the Lennard-Jones (L-J) potential,^{26,27} and the electrostatic interaction is modeled using Coulomb's law

$$\phi(r_{ij}) = 4\epsilon_{\text{oo}} \left[\left(\frac{\sigma_{\text{oo}}}{r_{\text{oo}}} \right)^{12} - \left(\frac{\sigma_{\text{oo}}}{r_{\text{oo}}} \right)^6 \right] + \frac{1}{4\pi\epsilon_0} \sum_{i=1}^3 \sum_{j=1}^3 \frac{q_i q_j}{r_{ij}} \quad (1)$$

where the L-J potential is applied only for the oxygen–oxygen interaction, with $\sigma_{\text{oo}} = 3.166 \text{ \AA}$ and $\epsilon_{\text{oo}} = 0.6502 \text{ kJ/mol}$. The last term in eq 1 describes the Coulomb force between charged atoms, where q_i is the charge on atom i , r_{ij} is the distance between atoms i and j , and ϵ_0 is the dielectric constant of vacuum. In the present study, it is normalized to 1.

An ionically conducting nanodroplet is made of pure water and Na^+/Cl^- ions. To calculate the interaction between the ions, the following Huggins–Mayer²⁸ potential was employed,

$$\phi(r_{ij}) = \frac{z_i z_j e^2}{r_{ij}} + A_{ij} b_{ij} \exp\left(\frac{\sigma_i + \sigma_j - r_{ij}}{\rho}\right) - \frac{C_{ij}}{r_{ij}^6} - \frac{D_{ij}}{r_{ij}^8} \quad (2)$$

where z_i is the formal ionic charge of ionic species i , e is the fundamental unit of electronic charge, ρ is the scale parameter associated with the system, and A_{ij} , B_{ij} , C_{ij} , and D_{ij} are adjustable parameters. The potential is a function of the particle types and the distance between them, r_{ij} . The first term represents the Coulombic interaction between two ions, and the latter terms represent a combination of the dispersion forces and repulsive forces. Table 1 gives potential parameters of the ion–ion interaction.

The usual modified L-J potential and the combining rules are used to determine interactions among solid atoms, ions, and water molecules. Bateni et al.^{29,30} has set up an experiment in which the drop was placed between insulated capacitor plates. This is imitated by exposing the system to a uniform external field.^{13,15,17,25} When an external electric field E is present, an additional force $f_{ie} = q_i E$ is exerted on each atom according to its charge q_i . Details of the treatment are given in the literature.³¹

The solid substrate consists of 10 816 solid atoms arranged in a diamond cubic lattice with a lattice constant of 5.46 \AA . This is

one of the solid silicon structures. Figure 1 shows the MD simulation ensemble. The solid substrate is rigid. The droplet

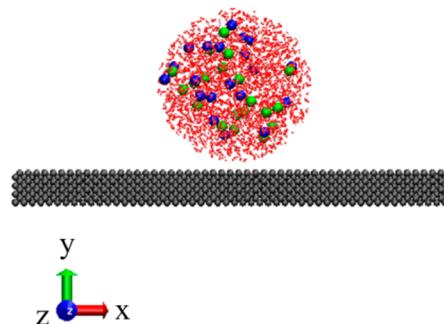


Figure 1. Initial structure of the ensemble.

has 2000 water molecules stacked in a spherical droplet of radius 2.5 nm and is large enough for an MD simulation.¹⁶ The size of the simulation box was set as $140 \times 140 \times 140 \text{ \AA}^3$. We study NaCl solutions at concentrations of 0.0268, 0.1339, 0.2678, 0.4017, 0.5356, 0.8034, and 1.071 M ($1 \text{ M} = 1 \text{ mol/dm}^3$) with the corresponding number of Na^+/Cl^- pairs being 1, 5, 10, 15, 20, 30, and 40, respectively.

The LAMMPS molecular dynamics code³² was used to carry out computer simulations in the NVT ensemble. The initial velocities are assigned to the atoms randomly according to the system's temperature of 300 K . The Nose–Hoover thermostat,³³ which relaxes the temperature in a timespan of 100 time steps, was used at every time step to make sure that the ensemble is kept at the desired temperature. The time step is 2 fs with the Verlet integration scheme for velocity. Because the droplet has a finite size and the solid substrate carries no charges, the use of Ewald sums is not needed.^{11,24} All of the interaction calculations are truncated smoothly at 15.0 \AA .

Periodic boundary conditions are applied along the x and z (i.e., parallel) directions. In the present study, when the distance between ions on different edges is smaller than the cutoff radius, all of the interaction forces between ions are set to zero regardless of the dispersion or repulsion force. In the y (i.e., vertical) direction, the mirror boundary condition is specified at the top surface; that is, if the atom reaches the boundary, the x - and z -velocity components remain the same while its y -velocity component changes sign. The bottom surface of the box is fixed to the solid surface.

The system was allowed to run for up to 200 000 time steps to ensure a good equilibrium state. Afterward, a sample was taken every 50 time steps to obtain the statistically equilibrium averaged values in the next 50 000 time steps. Then an external electric field was imposed in the x direction parallel to the plate (as shown in Figure 1). An additional 100 000 time steps were used for the system to reach a new equilibrium state, and afterward a sample is taken for analysis as above.

In the presence of an external electric field, the shape of a water droplet on the plate is more like part of ellipsoid than a

spherical crown.¹¹ Details of the contact angle calculation have been given in our previous studies.¹⁶

3. RESULTS AND DISCUSSION

3.1. Effect of NaCl Concentration. MD simulations were carried out for a droplet of various ion concentrations in the absence of an imposed field. The calculated equilibrium contact angles are plotted in Figure 2 as a function of the ion

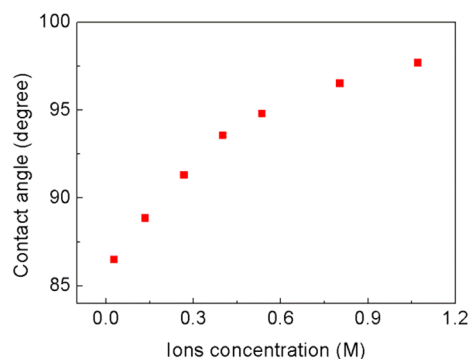


Figure 2. Effect of ion concentration on the equilibrium contact angle of an ionized droplet spreading on solid surface in the absence of an electric field.

concentration. It is known that a droplet of pure water wets the pure silicon solid substrate at a contact angle of 86.4° .¹⁶ As shown in Figure 2, the contact angle is increased considerably in the presence of Na^+ and Cl^- ions. Indeed, it is about 10° larger with a NaCl concentration of 1.071 M than with pure water. This is consistent with the reported work, in which contact angles were measured for NaCl and MgCl_2 solutions.²⁵ Measurements and model calculations for a molecularly heterogeneous TiO_2 /OTHS surface suggest a weak decrease in contact angle upon the addition of salt.³⁴ This reduction results primarily from the absorption of ions onto the strongly polar TiO_2 patches, which increases the solid surface wettability and hence causes the contact angle to decrease. On a silicon surface, however, the solid surface attraction is not strong enough to capture the ion absorbed as firmly as in the case of TiO_2 ; as a result, the contact angle increases.

3.2. Effect of Electric Field. The effect of the field applied perpendicularly to the solid surface with respect to the contact angle of Na^+/Cl^- ionic liquids has been analyzed;²⁵ here the focus is on the effect of the electric field parallel to the solid surface. The MD simulations were carried out with electric field strengths of 0.05 and 0.1 V/Å. Figure 3 shows the equilibrium states for the spreading of ionically conducting water droplets of two different Na^+/Cl^- ion concentrations (i.e., 0.0268 and 0.8034 M). Figure 4 depicts the equilibrium leading and trailing contact angles as a function of Na^+/Cl^- ion concentration for different electric field strengths. Clearly, the asymmetry of the leading and trailing contact angles depends on both the electric field strength and the ion concentration. With an electric field strength of 0.05 V/Å, the ionically conducting water droplet spreads asymmetrically on the solid silicon surface with the leading contact angle being larger than the trailing one. The asymmetry disappears and the leading and trailing contact angles become essentially the same as the ion concentration increases and exceeds 0.4 M. However, with the electric field increased to 0.1 V/Å, the salty droplet spreads symmetrically regardless of the ion concentrations. In fact, it wets the solid

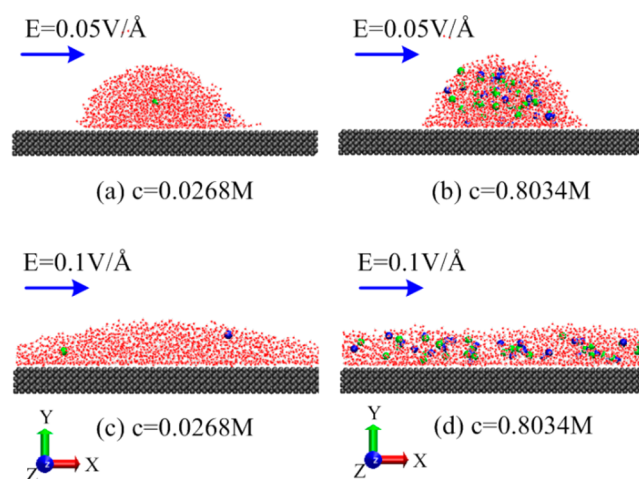


Figure 3. Equilibrium shapes of an ionized water droplet as it is spreading on a solid surface in the presence of a parallel electric field.

surface completely (the equilibrium contact angle equals 0°) as the Na^+/Cl^- concentration is increased beyond 0.2678 M. These results suggest that the electrowetting of an ionically conducting droplet can be manipulated by controlling either the ion concentration or the applied field strength or both.

The Na^+/Cl^- ions are distributed randomly in a water droplet in the initial state. In the case of a low ion concentration ($c = 0.0268$ M), there is only one pair of Na^+/Cl^- ions in the water droplet. More simulations were applied to determine whether the position of ions affects the electrically induced spreading behavior. Different from the general procedure described above, more than 50 000 time steps were first run to make the system reach another equilibrium state. Afterward, external electric fields of 0.05 and 0.1 V/Å were imposed on system. A sample was taken for analysis after the electrically induced spreading reached a new equilibrium state. The results show that the electrically induced spreading of a water droplet in a different initial state reached the same equilibrium state with the same contact angle distribution. This indicates that the initial position of ions does not affect the droplet spreading behavior.

3.3. Dynamic Spreading Process. To gain physical insight into the fundamental mechanism governing the electrospreeding of ionically conducting droplets, the dynamic spreading process of droplets with ion concentrations of 0.2678 and 0.8034 M is examined for an electric field of 0.1 V/Å. For these calculations, the droplet was first allowed to spread to an equilibrium state without an applied electric field. Then an electric field of 0.1 V/Å, parallel to the solid substrate, was introduced. Figure 5 displays a set of snapshots of the droplet spreading dynamics, and the corresponding dynamic contact angles are plotted in Figure 6. The dynamic contact angles are obtained as the average values for some snapshots around a time point. An inspection of Figures 5 and 6 indicates that with an ion concentration of 0.2678 M the application of an electric field immediately deforms and spreads the droplet asymmetrically, with the leading contact angle being larger than the trailing one. The asymmetric spreading continues until a time point of $t = 600$ ps is reached. Then the deformation gradually becomes symmetric and remains so afterward until the final equilibrium state is reached. For both cases, the droplets completely wet the solid surface at the final equilibrium (Figure 4). These dynamic spreading phenomena that involve the

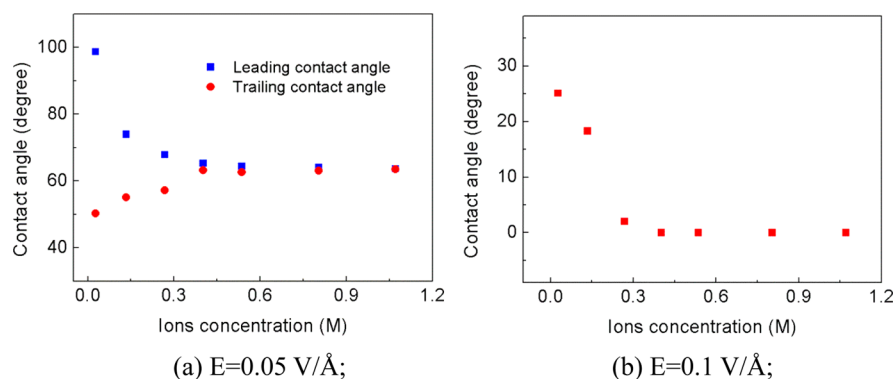


Figure 4. Equilibrium contact angles as a function of ion concentration for electric fields of 0.05 and 0.1 V/Å.

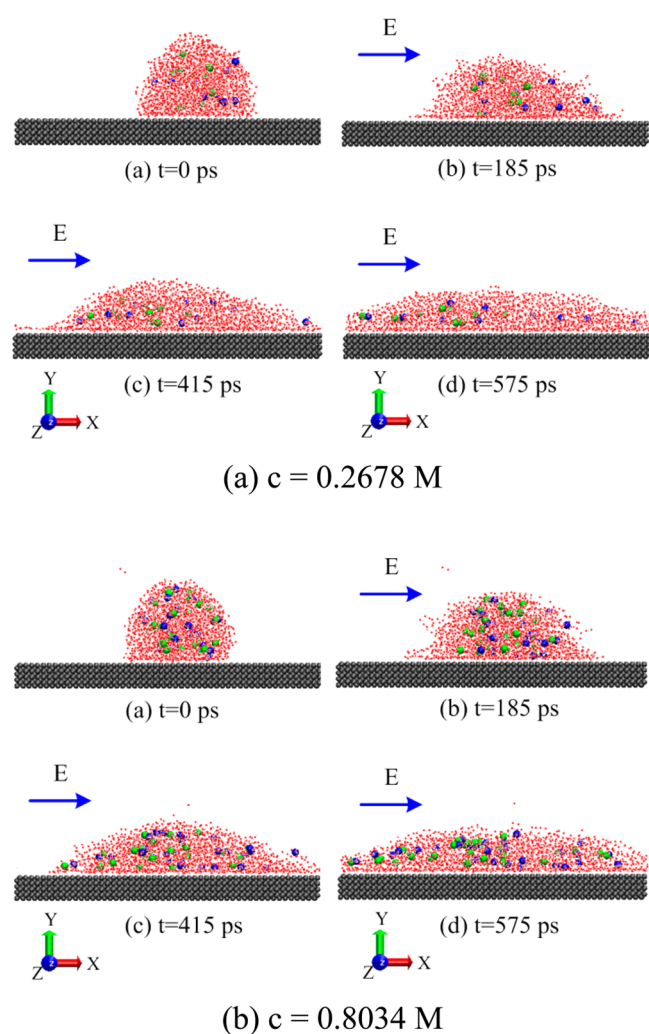


Figure 5. Dynamic spreading of a water droplet on a solid surface under the influence of an electric field ($E = 0.1 \text{ V/Å}$).

asymmetric-to-symmetric transition are also observed in other cases with ion concentrations of $<0.2678 \text{ M}$, and the details were omitted here for simplicity. For a higher ion concentration (i.e., 0.8034 M), the droplet spreads symmetrically on the same solid surface all the time, as illustrated in Figures 5b and 6b. The contact angle decreases monotonously until the droplet completely wets the solid surface.

Responding to the applied electric field, water molecules are classified as electric dipoles. They rotate and realign themselves

with hydrogen atoms along the electric field direction and oxygen atoms in the opposite direction. Ions in water droplets interact with hydrogen and oxygen atoms and affect their rotation and realignment, acting as a blending agent. This effect is further enhanced as the ion concentration increases. With a lower ion concentration, the droplet spreads asymmetrically, similar to that with a droplet of pure water, the main difference being that for the latter, the leading contact angle experiences a brief increase before starting to decline.

3.4. Profile of Interfacial Water Dipole Moment Vector

Because they are polar in nature, water molecules tend to realign themselves, in response to an applied electric field. These movements can be restricted near a solid–liquid interface. There, the competition between the electric field force and the force relative to the solid surface determines the motion of the water molecules. This competing mechanism is further complicated by the presence of additional ions in the aqueous solutions. Because there is considerable fluctuation in the molecular dynamic simulation at the three-phase interface, it is difficult to calculate the water dipole moment vector in this area. Thus, only water molecules at the solid–liquid interface were used to calculate the dipole moment vector. Figure 7 shows the distribution of the dipole moment vector μ as a function of the angles between the dipole vector and the solid surface. As expected, the distribution of μ peaks at dipole orientations parallel to the interface. MD simulations²⁵ indicate that there is essentially no ion adsorption on the nonpolar surface and between the first ionic layers and on the solid surface there is a layer of water molecules. In a weak electric field ($E = 0.05 \text{ V/Å}$), the dipole moment vector distribution profile remains practically the same for all ion concentrations. In contrast, with a strong electric field ($E = 0.1 \text{ V/Å}$), some ions move to the solid–liquid interface and cause the dipole moment in this area to increase with an increase in ion concentration. Some ions move to the droplet interface area and affect the contact line, which helps to stretch the contact surface. As a result, the ionically conducting droplet completely wets the solid surface. Clearly, for the case under study, complete wetting is due not only to the presence of more ions pulling the contact line and stretching the contact surface but also to the interaction between water molecules and ions when the electric force induces these ions to move.

3.5. Motion of Ions During Electrowetting. A pure water droplet spreads asymmetrically with a smaller electric field of 0.05 V/Å , and it undergoes the transition from asymmetric to symmetric spreading with a stronger electric field of 0.1 V/Å . For an ionically conducting droplet, such as

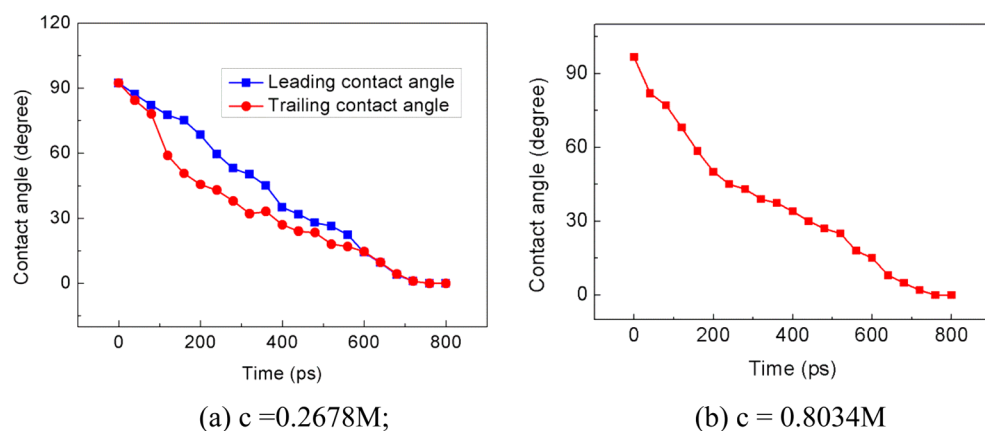


Figure 6. Evolution of the dynamic contact angles during the electrically induced spreading of ionically inducing water droplets of different ion concentrations ($E = 0.1 \text{ V/\AA}$).

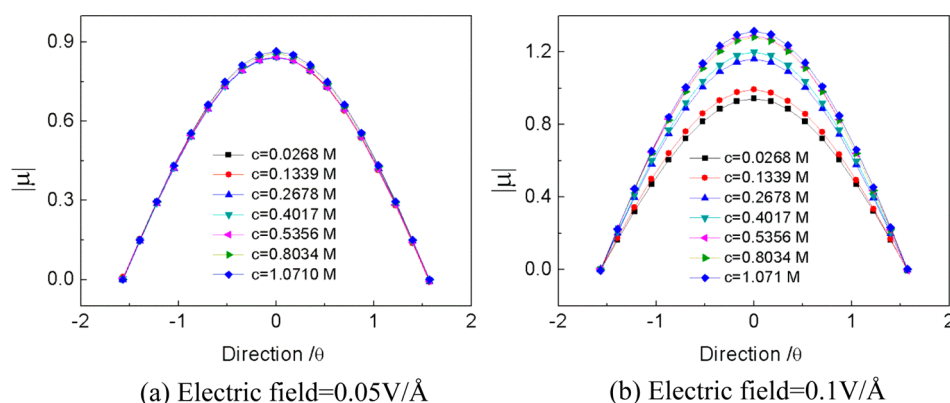


Figure 7. Distribution of the water dipole moment vector in the solid/liquid interface area.

that containing the Na^+/Cl^- ions, both the ion concentration and the electric field can affect the spreading behavior. Understanding the motion of ions in an electric field helps to elucidate the microscopic mechanism governing the electro-wetting processes.

The Na^+/Cl^- ions are randomly distributed in the droplet with similar trajectories during electrically induced spreading. Thus, one Na^+ and one Cl^- were chosen to describe the moving properties. Figures 8 and 9 depict moving trajectories of the Na^+/Cl^- ions during droplet spreading with applied electric fields of 0.05 and 0.1 V/\AA . The ion concentrations of 0.0268 and 0.5356 M were considered. Once again, both the ion concentration and the electric field strength play important roles in governing the motion of Na^+/Cl^- ions during droplet spreading. With an electric field of 0.05 V/\AA (Figure 8), the ions tend to spread in the direction of the applied electric field. However, the spreading is very small and the trajectories of ions undergo considerable fluctuation. As shown in Figure 8, the ions move about 15 \AA in the electric field direction during the whole spreading process. In the direction perpendicular to the electric field, the trajectory of the Cl^- ion shows a fluctuation of about 20 \AA . This is because the effect of a relatively weak electric field is roughly balanced by the interaction among water molecules. Consequently, the effects of the electric field on the spreading behavior and contact angle are rather small, even though the ions have a tendency to spread in the presence of a weak electric field. The contact angle was determined by the competition between the electric force and the interaction among water molecules, ions, and the solid surface. Thus, for

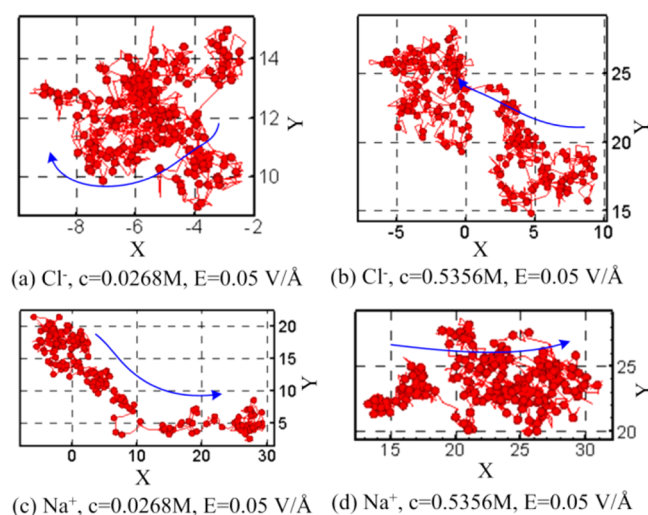


Figure 8. Moving trajectories for ions in the droplet (with ion concentrations of $c = 0.0268$ and 0.5356 M) spreading as affected by the electric field ($E = 0.05 \text{ V/\AA}$).

the present case, the contact angle remains practically the same with the increasing ion concentration for the electric field E up to 0.05 V/\AA . When the applied electric field strength is increased to 0.1 V/\AA (Figure 9), the Na^+/Cl^- ions move along the direction of the electric field force with only a small fluctuation. It is also observed that some ions may escape from the boundary during spreading with a parallel electric field of

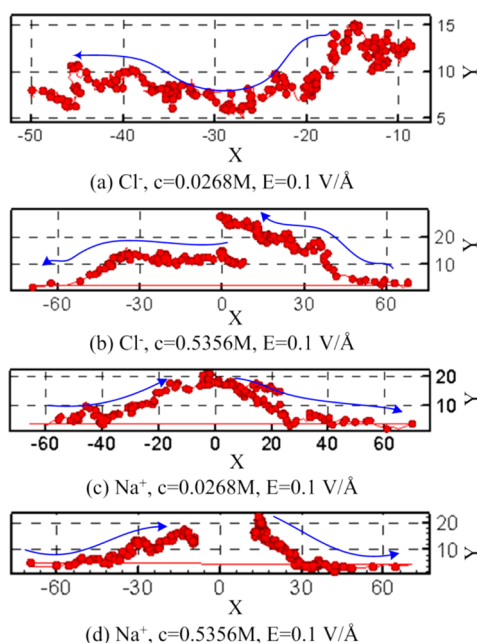


Figure 9. Moving trajectories for ions in the droplet (with ion concentrations of $c = 0.0268$ and 0.5356 M) spreading as affected by the electric field ($E = 0.1$ V/Å).

0.1 V/Å. In our simulation system, the x direction is a periodic boundary condition, so the ions evaporate from one side and will enter the droplet from another side. The literature²⁵ reports that a field of magnitude >0.08 V/Å perpendicular to the surface is sufficient to cause ion evaporation.

4. CONCLUDING REMARKS

This article has presented an MD study of the combined effect of the electric field and the ion concentration on the spreading of an ionically conducting water droplet on a solid substrate. Polar water molecules interact with the applied electric field and reorient their point dipoles. The reorientation is further affected by the presence of freely moving cations and anions. The ions in the solution cause the contact angle to increase in the absence of an electric field. For a droplet with an ion concentration of 1.071 M, the equilibrium contact angle is increased by 10° . For the electric field applied parallel to the solid surface, the static contact angle of the ionically conducting liquid is affected by both the field strength and the ion concentration. In a parallel electric field of 0.05 V/Å, a droplet with a low ion concentration spreads asymmetrically, with the leading contact angle being larger than the trailing one. This asymmetry of contact angles gradually diminishes as the ion concentration increases to 0.4 M; at and beyond this point, the droplet spreading becomes symmetric. For a higher electric field of 0.1 V/Å, the dynamic spreading of an ionically conducting water droplet of low ion concentration (i.e., 0.2678 M) undergoes an asymmetric-to-symmetric transition similar to that of a pure water droplet. For a high ion concentration, spreading remains symmetric and the droplet completely wets the solid surface at equilibrium. Though spreading is determined by a competing mechanism between the applied electric field and the intermolecular forces, the additional ions, acting as a blending agent, interact with hydrogen and oxygen atoms and play an important role in the electrowetting of an ionically conducting droplet.

AUTHOR INFORMATION

Corresponding Authors

*E-mail: benqli@umich.edu. Tel: (+1)313-593-5241. Fax: (+1)313-593-3851.

*E-mail: liuchao@cqu.edu.cn. Tel: (+86)023-65112469. Fax: (+86) 023-65112469.

Author Contributions

The manuscript was written through the contributions of all authors. All authors have given approval to the final version of the manuscript.

Notes

The authors declare no competing financial interest.

ACKNOWLEDGMENTS

We acknowledge the financial support of this work from the Oak Ridge University Research Alliance of the Department of Energy and Research Fund for the Doctoral Program of Higher Education (no. 20090191110016).

REFERENCES

- (1) Blake, T. D.; Clarke, A.; Coninck, J. D.; Ruijter, M. J. Contact Angle Relaxation during Droplet Spreading: Comparison between Molecular Kinetic Theory and Molecular Dynamics. *Langmuir* **1997**, *13*, 2164–2166.
- (2) Ingebrigtsen, T.; Toxvaerd, S. Contact Angle of Lennard-Jones Liquids and Droplets on Planar Surface. *J. Phys. Chem. C* **2007**, *111*, 8518–8523.
- (3) Guo, H. K.; Fang, H. P. Drop Size Dependence of the Contact Angle of Nanodroplets. *Chin. Phys. Lett.* **2005**, *22*, 787–790.
- (4) Bertrand, E.; Blake, T. D.; Coninck, J. D. Influence of Solid-liquid Interactions on Dynamic Wetting: a Molecular Dynamics Study. *J. Phys.: Condens. Mater.* **2009**, *21*, 464124.
- (5) Nieminen, J. A.; Abraham, D. B.; Karttunen, M.; Kaski, K. Molecular Dynamics of a Microscopic Droplet on Solid Surface. *Phys. Rev. Lett.* **1992**, *69*, 124–127.
- (6) Shi, B.; Dhir, V. K. Molecular Dynamics Simulation of the Contact Angle of Liquids on Solid Surface. *J. Chem. Phys.* **2009**, *130*, 034705 (5pp).
- (7) Ohler, B.; Langel, W. Molecular Dynamics Simulations on the Interface between Titanium Dioxide and Water Droplets: A New Model for the Contact Angle. *J. Phys. Chem. C* **2009**, *113*, 10189–10197.
- (8) Ku, B. K.; Kim, S. S. Electro Hydrodynamic Spraying Characteristics of Glycerol Solutions in Vacuum. *J. Electrostat.* **2003**, *57*, 109–128.
- (9) Barletta, M.; Gisario, A. Electrostatic Spray Painting of Carbon Fibre-Reinforced Epoxy Composites. *Prog. Org. Coat.* **2009**, *64*, 339–349.
- (10) Twardeck, T. G. Effect of Parameter Variations on Drop Placement in an Electrostatic Ink Jet Printer. *IBM J. Res. Dev.* **1977**, *21*, 31–36.
- (11) Schaffer, E.; Albrecht, T. T.; Russell, T. P.; Steiner, U. Electrically Induced Structure Formation and Pattern Transfer. *Nature* **2000**, *403*, 874–877.
- (12) Liang, X. G.; Zhang, W.; Li, M. T.; Xia, Q. F.; Wu, W.; Ge, H. X.; Huang, X. Y.; Chou, S. Y. Electrostatic Force-Assisted Nanoimprint Lithography (EFAN). *Nano Lett.* **2005**, *05*, 527–530.
- (13) Daub, C. D.; Bratko, D.; Leung, K.; Luzar, A. Electrowetting at the Nanoscale. *J. Phys. Chem. C* **2007**, *111*, 505–509.
- (14) Bratko, D.; Daub, C. D.; Leung, K.; Luzar, A. Effect of Field Direction on Electrowetting in a Nanopore. *J. Am. Chem. Soc.* **2007**, *129*, 2504–2510.
- (15) Bratko, D.; Daub, C. D.; Luzar, A. Water-Mediated Ordering of Nanoparticles in an Electric Field. *Faraday Discuss.* **2009**, *141*, 55–66.

- (16) Song, F. H.; Li, B. Q.; Liu, C. Molecular Dynamics Simulation of Nanosized Water Droplet Spreading in an Electric Field. *Langmuir* **2013**, *29*, 4266–4274.
- (17) Yen, T. H. Investigation of the Effects of Perpendicular Electric Field and Surface Morphology on Nanoscale Droplet Using Molecular Dynamics Simulation. *Mol. Simul.* **2012**, *38*, 509–517.
- (18) Wijethunga, P. A. L.; Nanayakkara, Y. S.; Kunchala, P.; Armstrong, D. W.; Moon, H. On-Chip Drop-to-Drop Liquid Microextraction Coupled with Real-Time Concentration Monitoring Technique. *Anal. Chem.* **2011**, *83*, 1658–1664.
- (19) Amin, A. A.; Jagtiani, A.; Vasudev, A.; Hu, J.; Jiang, Z. Soft Microgripping Using Ionic Liquids for High Temperature and Vacuum Applications. *J. Micromech. Microeng.* **2011**, *21*, 125025.
- (20) Nanayakkara, Y. S.; Moon, H.; Armstrong, D. W. A Tunable Ionic Liquid Based RC Filter Using Electrowetting: A New Concept. *ACS Appl. Mater. Interfaces* **2010**, *2*, 1785–1787.
- (21) Hu, X.; Zhang, S.; Qu, C.; Zhang, Q.; Lu, L.; Ma, X.; Zhang, X.; Deng, Y. Ionic Liquid Based Variable Focus Lenses. *Soft Matter* **2011**, *7*, 5941–5943.
- (22) Paneru, M.; Priest, C.; Sedev, R.; Ralston, J. Static and Dynamic Electrowetting of an Ionic Liquid in a Solid/Liquid/Liquid System. *J. Am. Chem. Soc.* **2010**, *132*, 8301–8308.
- (23) Paneru, M.; Priest, C.; Sedev, R.; Ralston, J. Electrowetting of Aqueous Solutions of Ionic Liquid in Solid–Liquid–Liquid Systems. *J. Phys. Chem. C* **2010**, *114*, 8383–8388.
- (24) Li, H.; Paneru, M.; Sedev, R.; Ralston, J. Dynamic Electrowetting and Dewetting of Ionic Liquids at a Hydrophobic Solid–Liquid Interface. *Langmuir* **2013**, *29*, 2631–2639.
- (25) Daub, C. D.; Bratko, D.; Luzar, A. Electric Control of Wetting by Salty Nanodrops: Molecular Dynamics Simulations. *J. Phys. Chem. C* **2011**, *115*, 22393–22399.
- (26) Berendsen, H. J. C.; Grigera, J. R.; Straatsma, T. P. The Missing Term in Effective Pair Potentials. *J. Phys. Chem.* **1987**, *91*, 6269–6271.
- (27) Kirby, B. J. *Micro- and Nanoscale Fluid Mechanics: Transport in Microfluidic Devices*; Cambridge University Press: New York, 2010.
- (28) Reagan, M. T.; Harris, J. G.; Tester, J. W. Molecular Simulations of Dense Hydrothermal NaCl-H₂O Solutions from Subcritical to Supercritical Conditions. *J. Phys. Chem. B* **1999**, *103*, 7935–7941.
- (29) Bateni, A.; Susnar, S. S.; Amirfazali, A.; Neumann, A. W. Development of a New Methodology to Study Drop Shape and Surface Tension in Electric Fields. *Langmuir* **2004**, *20*, 7589–7597.
- (30) Bateni, A.; Laughton, S.; Tavana, H.; Susnar, S. S.; Amirfazali, A.; Neumann, A. W. Effect of Electric Fields on Contact Angle and Surface Tension of Drops. *J. Colloid Interface Sci.* **2005**, *283*, 215–222.
- (31) Park, S.; Schulten, K. Calculating Potentials of Mean Force from Steered Molecular Dynamics Simulations. *J. Chem. Phys.* **2004**, *120*, 5946–5961.
- (32) Plimpton, S. J. Fast Parallel Algorithms for Short-Range Molecular Dynamics. *J. Comput. Phys.* **1995**, *117*, 1–19.
- (33) Hünenberger, P. H. Thermostat Algorithms for Molecular Dynamics Simulations. *Adv. Polym. Sci.* **2005**, *173*, 105–149.
- (34) Hanly, G.; Fornasiero, D.; Ralston, J.; Sedev, R. Electrostatics and Metal Oxide Wettability. *J. Phys. Chem. C* **2011**, *115*, 14914–14921.
- (35) Sakuma, H.; Kawamura, K. Structure and Dynamics of Water on Li⁺, Na⁺, K⁺, Cs⁺, H₃O⁺ Exchanged Muscovite Surfaces: A Molecular Dynamics Study. *Geochim. Cosmochim. Acta* **2011**, *75*, 63–81.